

⁷Rogers, C. A., "Dynamic and Structural Control Utilizing Smart Materials and Structures," *Proceedings of the International Workshop on Intelligent Materials*, Tsukuba, Japan, 1989, pp. 109–121.

⁸Bramwell, A. R. S., *Helicopter Dynamics*, Arnold, London, 1976, pp. 154, 155.

⁹Popescu, B., and Giurgitiu, V., "The Calculation and Design of the Oscillating Rotor," (in Romanian), STRAERO S.A., TR N-6076, Bucharest, Romania, June 1991.

¹⁰Friedmann, P. P., Hammond, C. E., and Tze-Hsin, W., "Efficient Numerical Treatment of Periodic Systems with Application to Stability Problems," *International Journal for Numerical Methods in Engineering*, Vol. 11, No. 7, 1977, pp. 1118–1122.

Turbulence Model Evaluation for Use with Supercritical Airfoils

W. Kelly Londenberg*

ViGYAN, Inc.,

Hampton, Virginia 23666

Nomenclature

- C_p = pressure coefficient
- c = chord
- c_l = sectional lift coefficient
- M = corrected Mach number
- R_N = Reynolds number based on chord
- x/c = nondimensional chord station
- y^+ = law of the wall coordinate
- α = angle of attack, deg
- δ_a = aileron deflection, deg

Introduction

INCREASING the efficiency of aircraft configurations in general, and transport aircraft in particular, is a never-ending task. With progress being made in the optimization of the cruise configuration of transport aircraft, efforts are now being made to increase the performance at off-design conditions, such as when ailerons are deflected, high-lift configurations, and near the buffet boundary. Small decreases in drag coefficient at off-design conditions can make significant improvements in the overall performance of the vehicle. For example, a 1% increase in takeoff L/D is equivalent to a 2800-lb increase in payload, or a 150-nm increase in range for a typical large, twin-engine transport.¹ Any analysis or wind-tunnel testing of these viscous dominated flowfields must be done at conditions where the boundary-layer thickness and state are simulated. Since Reynolds number effects on aerodynamic data is not a linear function, this must be made at full-scale Reynolds number conditions to correctly simulate the boundary-layer profiles.

With the continuing advancement of computing power and algorithm efficiency, it has become more practical to calculate flows around aerospace vehicles at full-scale Reynolds number conditions. The use of the computer allows for the identification of problem areas, and therefore, the streamlining of the wind-tunnel test program. At cruise conditions, the flow is nonseparated and can easily be computed using full potential or Euler methods coupled with boundary-layer tech-

niques. However, at off-design conditions, the flow may become separated and these simpler methods cannot accurately predict the flowfield. At these conditions Navier-Stokes solvers are required to predict the often complicated viscous-inviscid interactions that are occurring. Even with the increases in computer power and algorithm efficiency of recent years, turbulence quantities cannot yet be calculated directly, requiring the use of modeling techniques.

This Note will describe the evaluation of turbulence models as used for the analysis of a transport airfoil with deflected aileron at high Reynolds numbers and transonic Mach numbers. The turbulence models evaluated are the Baldwin-Lomax algebraic model,² the Johnson-King half-equation model,³ and the Baldwin-Barth⁴ and Spalart-Allmaras⁵ one-equation models. The analysis code used is the NASA Langley thin layer Navier-Stokes solver CFL3D.⁶

Results and Discussion

Solutions were calculated for the McDonnell Douglas Aerospace—Transport Aircraft Unit's DLBA032 12.3% chord thick supercritical airfoil. Experimental data were obtained for this airfoil at the Institute for Aerospace Research (IAR) 15- × 60-in. transonic wind tunnel. Force and pressure data were obtained for a wide range of angles of attack at Mach numbers corrected for both floor and ceiling wall effects, as well as for sidewall boundary effects using Murthy's methodology⁷ of 0.716 at Reynolds number based on chord of 5, 15, and 25 million, and at $M = 0.747$ for $R_N = 15 \times 10^6$. Data was also obtained for aileron deflections ranging from -5 deg [trailing-edge up (TEU)] to +5 deg [trailing-edge down (TED)].

Based on a grid resolution study performed for this airfoil with nondeflected aileron at $\alpha = 1.2$ deg, $R_N = 15 \times 10^6$, and $M = 0.716$, it was determined that a C-grid with a mesh size of 289×65 (wraparound x radial) with an outer boundary extent of $20c$ yielded results of acceptable accuracy.⁸ Minimum spacing normal to the surface was $1.5 \times 10^{-6}c$, which resulted in y^+ values at one grid point off of the surface of near 1.

The computational grid at the trailing edge of the airfoil was found to have significant effects in the computed solutions. Varying the streamwise clustering at the trailing edge by 0.1% chord moved the location of the computed shock wave nearly 1% chord.⁸ The sensitivity of the supercritical airfoil flowfield to trailing-edge clustering observed in this study is also evident in a study by Yu et al.⁹ The streamwise clustering at the trailing edge of the airfoil selected for use in the present study was 0.1% c . The flowfield around the DLBA032 airfoil is also very sensitive to how the trailing edge is closed. Several methods of closing this blunt trailing edge (approximately 0.5% c thick at the trailing edge) were tried. The only method that worked with all the turbulence models was that of averaging the upper and lower surface trailing-edge points.

Solutions were obtained for the DLBA032 airfoil using the Baldwin-Lomax, Johnson-King, Baldwin-Barth, and Spalart-Allmaras turbulence models. The same mesh was used for all Reynolds numbers. The resulting maximum y^+ values ranged from near 0.5 for $R_N = 5 \times 10^6$ to slightly greater than 1 for $R_N = 25 \times 10^6$. Transition was fixed for the calculations at the experimental transition grit location: 15% c upper surface and 28% c lower surface for $R_N = 5 \times 10^6$, 10% c upper surface and 15% c lower surface for $R_N = 15 \times 10^6$, and free transition (leading edge in the computations) for $R_N = 25 \times 10^6$.

The general effect of turbulence model on computed pressure distribution is shown in Fig. 1 for the airfoil with nondeflected aileron, and in Fig. 2 for the airfoil with 2-deg aileron deflection. These solutions were obtained for $M = 0.716$, and $\alpha = 1.20$ deg for $\delta_a = 0$ deg, and $\alpha = 1.24$ deg for $\delta_a = 2$ deg. All models predict pressures that are generally in good agreement with experimental pressures for the nonde-

Presented as Paper 93-0191 at the AIAA 31st Aerospace Sciences Meeting and Exhibit, Reno, NV, Jan. 11–14, 1993; received March 1, 1993; revision received May 13, 1993; accepted for publication May 13, 1993. This paper is declared a work of the U.S. Government and is not subject to copyright protection in the United States.

*Research Engineer, 30 Research Drive. Member AIAA.

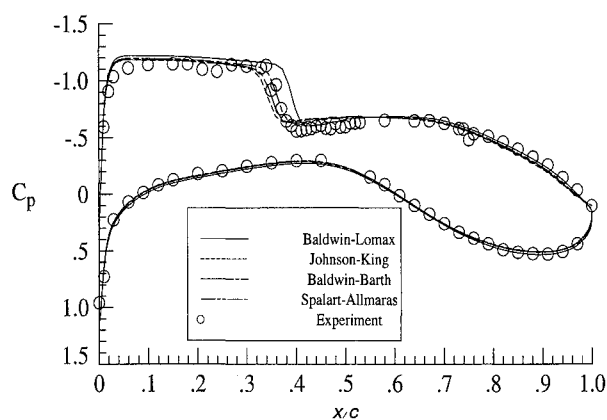


Fig. 1 Effect of turbulence model on pressure coefficients ($M = 0.716$, $R_N = 25 \times 10^6$, $\alpha = 1.21$ deg, $\delta_a = 0.0$ deg).

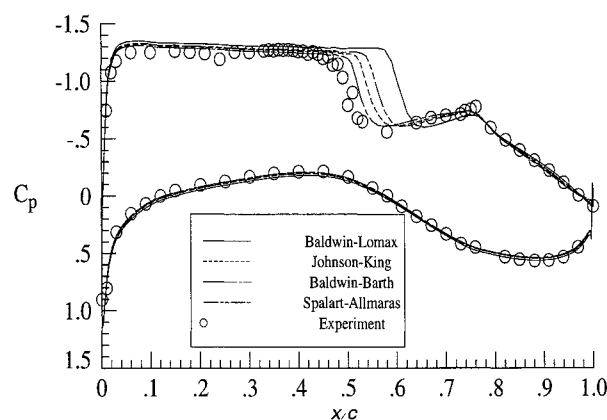


Fig. 2 Effect of turbulence model on pressure coefficients ($M = 0.716$, $R_N = 15 \times 10^6$, $\alpha = 1.23$ deg, $\delta_a = 2.0$ deg).

flected aileron case at 5, 15, and 25 million Reynolds number (only the $R_N = 25 \times 10^6$ case is shown here for brevity). However, when the aileron is deflected 2-deg down, all models predict a shock location that is downstream of experiment (Fig. 2). The three nonequilibrium models predict the shock location between 2–6% aft of experiment, with the Baldwin-Barth and Johnson-King models predictions closest to the experimental location. The Baldwin-Lomax equilibrium model predicts the shock location nearly 12% aft of experiment. Poorer comparisons with experiment were obtained for 5 and 25 million Reynolds numbers, although trends with Reynolds number were similar.⁸

Solutions obtained using each turbulence model predicted the expansions around the leading edge as well as over the hingeline well for all Reynolds numbers. The spikes in the pressure distribution at the trailing edge seen in Fig. 2 is a result of how the blunt trailing edge was closed for the calculations. Predicted lower surface pressures compare well with experiment, indicating that the wind-tunnel-corrected angle of attack is appropriate. Significant regions of separation were not predicted using any of the four turbulence models, which is consistent with experimental observations.

The effect of the Johnson-King and Baldwin-Barth turbulence models on the prediction of sectional lift coefficient is shown in Fig. 3. This comparison is being made only with these two turbulence models since pressure distributions predicted using the Baldwin-Lomax and Spalart-Allmaras turbulence models compared less favorably with experiment for the deflected aileron. The sectional lift coefficients predicted using these two models are similar for the nondeflected aileron case at all Reynolds numbers considered. Results compare well with experiment at the two higher Reynolds numbers,

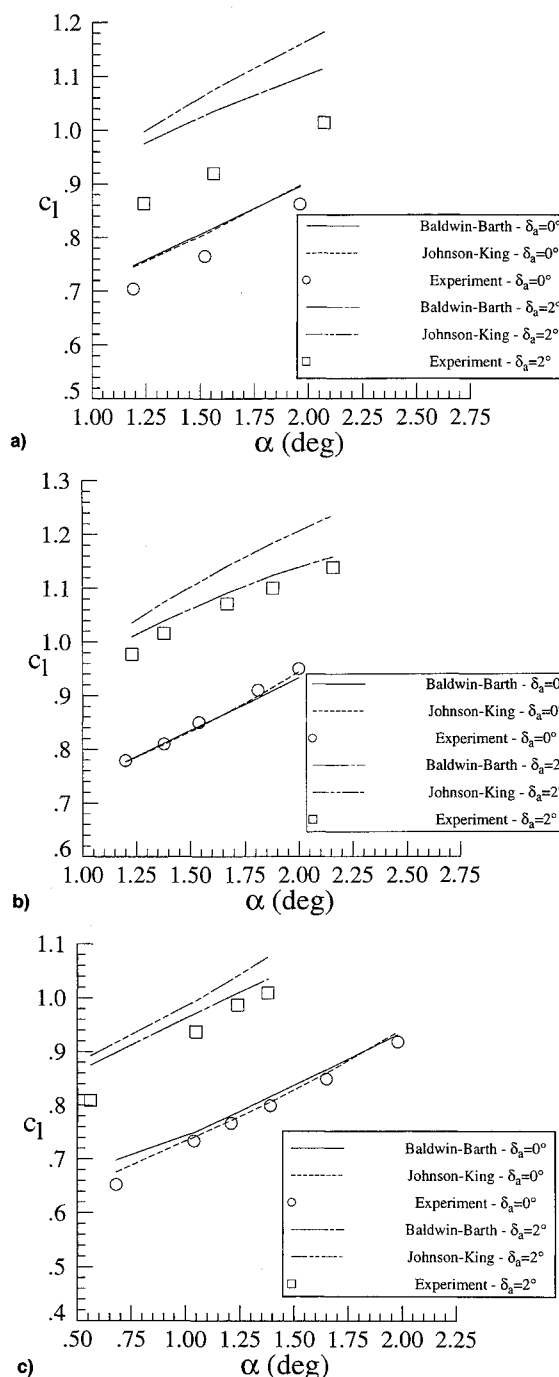


Fig. 3 Effect of turbulence model on sectional lift coefficient: a) $M = 0.716$, $R_N = 5 \times 10^6$; b) $M = 0.716$, $R_N = 15 \times 10^6$; and c) $M = 0.716$, $R_N = 25 \times 10^6$.

while c_l is overpredicted for $R_N = 5 \times 10^6$. Lift coefficient is overpredicted by both models at all three R_N for the deflected aileron, although results using the Baldwin-Barth model agree somewhat better.

Concluding Remarks

All turbulence models that were evaluated provided results that compared well with experiment for the nondeflected aileron geometry. However, the shock location was predicted 2–12% aft of the experimental location for $\delta_a = 2$ deg. The best results were obtained using the three nonequilibrium models for the deflected aileron geometry. The results predicted by the Baldwin-Barth turbulence model coupled with the CFL3D Navier-Stokes code yielded the best overall comparisons with experiment.

Acknowledgments

This research was sponsored, in part, by the National Aeronautics and Space Administration under Contract NAS1-18585. The author also acknowledges the assistance with using the CFL3D code and the various turbulence models made by Christopher Rumsey of NASA Langley Research Center. The experimental data was provided to NASA Langley Research Center by Frank Lynch of McDonnell Douglas Aerospace—Transport Aircraft Unit.

References

- ¹Garner, P. L., Meredith, P. T., and Stoner, R. C., "Areas for Future CFD Development as Illustrated by Transport Aircraft Applications," *Proceedings of the 10th AIAA Computational Fluid Dynamics Conference* (Honolulu, HI), AIAA, Washington, DC, 1991, pp. 10–20 (AIAA Paper 91-1527).
- ²Baldwin, B. S., and Lomax, H., "Thin-Layer Approximation and Algebraic Models for Separated Turbulent Flows," AIAA Paper 78-257, Jan. 1978.
- ³Abid, R., Vatsa, V. N., Johnson, D. A., and Wedan, B. W., "Prediction of Separated Transonic Wing Flows with Nonequilibrium Algebraic Turbulence Models," *AIAA Journal*, Vol. 28, No. 8, 1990, pp. 1426–1431.
- ⁴Baldwin, B. S., and Barth, T. J., "A One-Equation Turbulence Transport Model for High Reynolds Number Wall-Bounded Flows," NASA TM-102847, Aug. 1990.
- ⁵Spalart, P. R., and Allmaras, S. R., "A One-Equation Turbulence Model for Aerodynamic Flows," AIAA Paper 92-0439, Jan. 1992.
- ⁶Thomas, J. L., Taylor, S. L., and Anderson, W. K., "Navier-Stokes Computations of Vortical Flows over Low Aspect Ratio Wings," AIAA Paper 87-0207, Jan. 1987.
- ⁷Lynch, F. T., and Johnson, C. B., "Wind-Tunnel-Sidewall-Boundary-Layer Effects in Transonic Airfoil Testing—Some Correctable, but Some Not," AGARD-CP-429, Sept. 1987, pp. 18-1–18-16.
- ⁸Londenberg, W. K., "Turbulence Model Evaluation for the Prediction of Flows over A Supercritical Airfoil with Deflected Aileron at High Reynolds Number," AIAA Paper 93-0191, Jan. 1993.
- ⁹Yu, N. J., Allmaras, S. R., and Moschetti, K. G., "Navier-Stokes Calculations for Attached and Separated Flows Using Different Turbulence Models," AIAA Paper 91-1791, June 1991.

Direct Solution of the Aeroelastic Stability Equations

Maher N. Bismarck-Nasr*
*Instituto Tecnológico de Aeronáutica,
 São José dos Campos, SP 12228-900, Brazil*

Introduction

CURRENT aeroelastic analyses are performed through repetitive solutions of a complex eigenvalue problem or a determinant for a large number of reduced frequencies or velocities.^{1,2} The stability of the system is studied by numerically tracing the roots of the solutions in the traditional V - g - ω plots. The critical modes are then obtained from the crossing of the zero line of the real part of the roots (zero damping or flutter condition) and the imaginary part of the roots (zero frequency or divergence condition). The variants of the solutions can be separated into three main groups, namely the 1) p methods, 2) the k methods, and 3) the p - k methods. Many authors³ have discussed the difference between these

traditional solutions. While all these methods lead to approximately the same flutter and divergence speeds, they differ in the results obtained beyond the critical speeds. Classically, the display of the results in the form of V - g - ω diagrams is made on the implicit assumption that the shape of these plots reveal something about the severity of the instability beyond the critical speeds. Such interpretation must be made with great caution, since some of the solution variants, e.g., the classical k methods, can produce erroneous conclusions if interpretation about the damping obtained beyond the critical speeds is made.³ In many practical applications the main objective is the determination of the critical speeds and not the damping beyond these speeds. Examples are preliminary design and optimal design programs subjected to constraints on the critical aeroelastic velocities. In such conditions a rapid and automatic method for the evaluation of the least flutter and divergence speeds is required. In Ref. 4, it has been demonstrated that this end can be achieved when only in-quadrature air forces are considered in the nonstationary aerodynamic load formulation. In this Note, it is shown that in many cases where out-of-phase air loads are also considered, the problem can be cast into the solution of two equations, whose simultaneous solution determines directly the critical velocities and frequencies. Such applications include the formulations based on quasisteady aerodynamic theory and simple forms of unsteady aerodynamic loads.

Problem Formulation

The aeroelastic stability equations can be written in general form as

$$[p^2[M] + [K] - \Lambda[a(p)]]\{u\} = \{0\} \quad (1)$$

where $[M]$ is the mass matrix, $[K]$ is the stiffness matrix, Λ is an aerodynamic parameter function of the freestream velocity, and p is the problem eigenvalue, which is in general complex. The elements of the aerodynamic matrix, which are explicit functions of p , will depend on the theory used for the formulation of unsteady aerodynamic loads. In many cases, e.g., when the quasisteady aerodynamic theory or simple forms of unsteady aerodynamic loads are used, the matrix $[a(p)]$ assumes the simple form

$$[a(p)] = \gamma p[a_1] + [a_0] \quad (2)$$

where γ is an aerodynamic damping parameter, and the aerodynamic matrices $[a_1]$ and $[a_0]$ are real, with constant elements. Substituting Eq. (2) into Eq. (1), transforming the coordinates to the free vibration modal base, and using mode shapes normalized for the unit mass matrix, the aeroelastic stability equations read

$$[-p^2[I] + [\xi^2] - \Lambda[A_0] - i\gamma\Lambda p[A_1]]\{q_0\} = \{0\} \quad (3)$$

where solutions in the form

$$\{q\} = \{q_0\}e^{i\pi t} \quad (4)$$

have been considered for the modal amplitudes. Equation (3) represents a parametric eigenvalue problem whose characteristic equation can be written in general form as

$$p^{2n} + ic_1p^{2n-1} + c_2p^{2n-2} + \dots + c_{2n} = 0 \quad (5)$$

where n is the order of the system. Since the matrices of Eq. (3) are all real, it follows that the coefficients of the characteristic Eq. (5) are real and are functions of the aerodynamic parameter Λ and the damping factor γ . Now, on the borderline of stability, the roots p of Eq. (5) are real, so that we

Received Feb. 8, 1992; revision received Jan. 20, 1993; accepted for publication May 20, 1993. Copyright © 1993 by the American Institute of Aeronautics and Astronautics, Inc. All rights reserved.

*Professor, Division of Aeronautical Engineering. Member AIAA.